Supporting Information

Aggregation Behaviour of Biocompatible Choline Carboxylate Ionic Liquids and their Interactions with Biomolecule through Experimental and Theoretical Investigations

Somenath Panda,[1][†] Kaushik Kundu,[2, 3][†] Anusha Basaiahgari,[1] Akhil Pratap Singh,[1,2]

Sanjib Senapati,[2] and Ramesh L. Gardas[1]*

[1] *Department of Chemistry, Indian Institute of Technology Madras, Chennai 600036, India.*

[2] *Department of Biotechnology, Bhupat and Jyoti Mehta School of Biosciences, Indian Institute of Technology Madras, Chennai 600036, India.*

[3] Present address: *Department of Inorganic and Physical Chemistry, Indian Institute of Science, Bangalore 560012, India.*
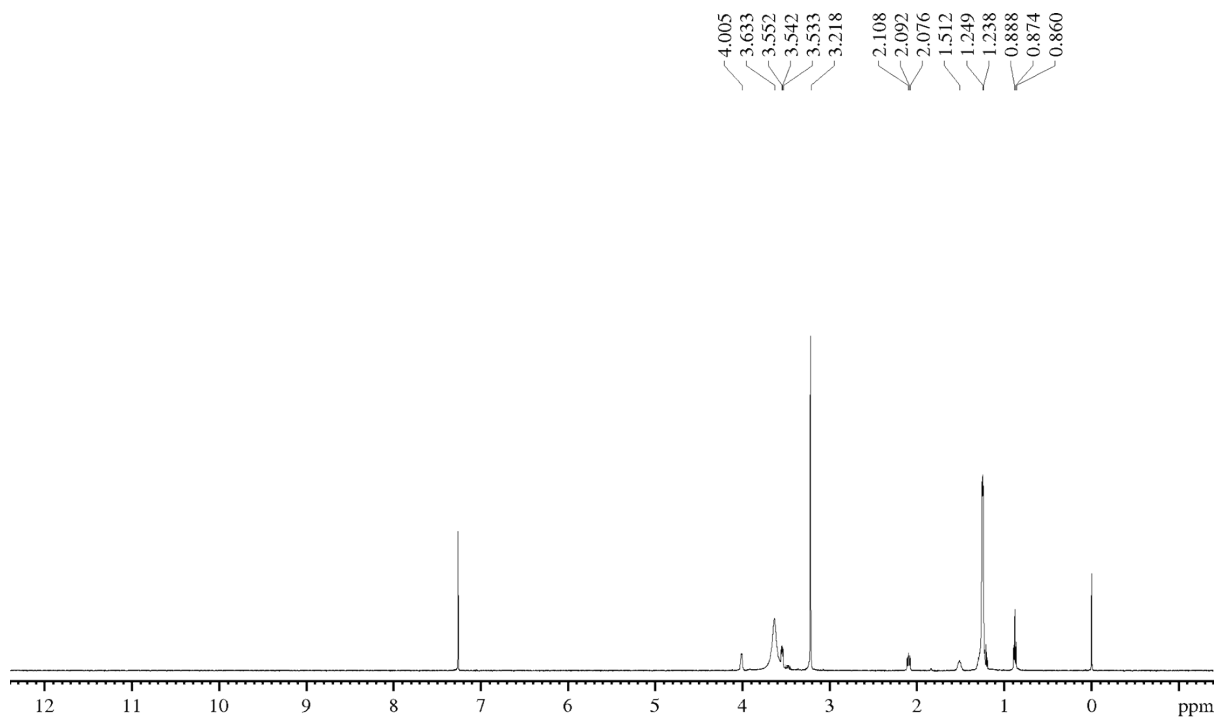
[†] S. P. and K. K have contributed equally to this work.
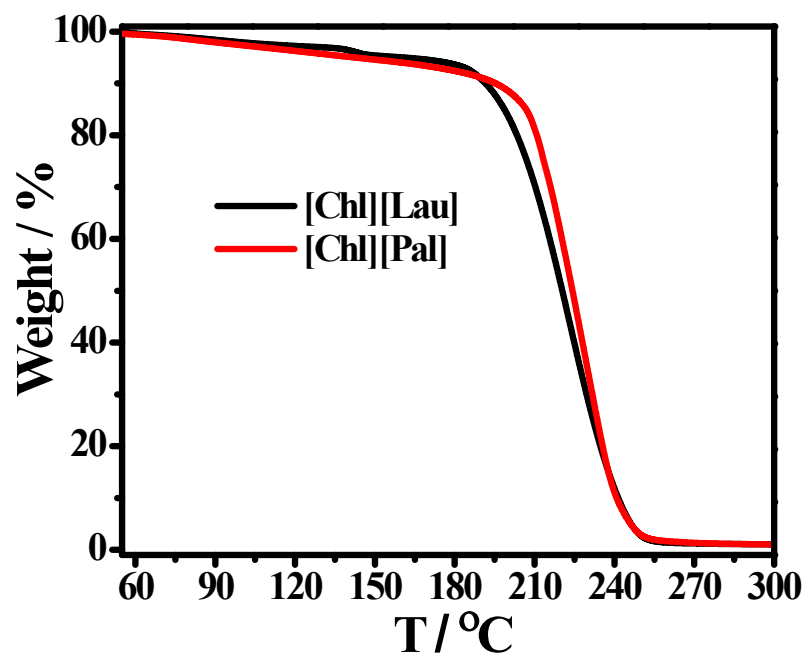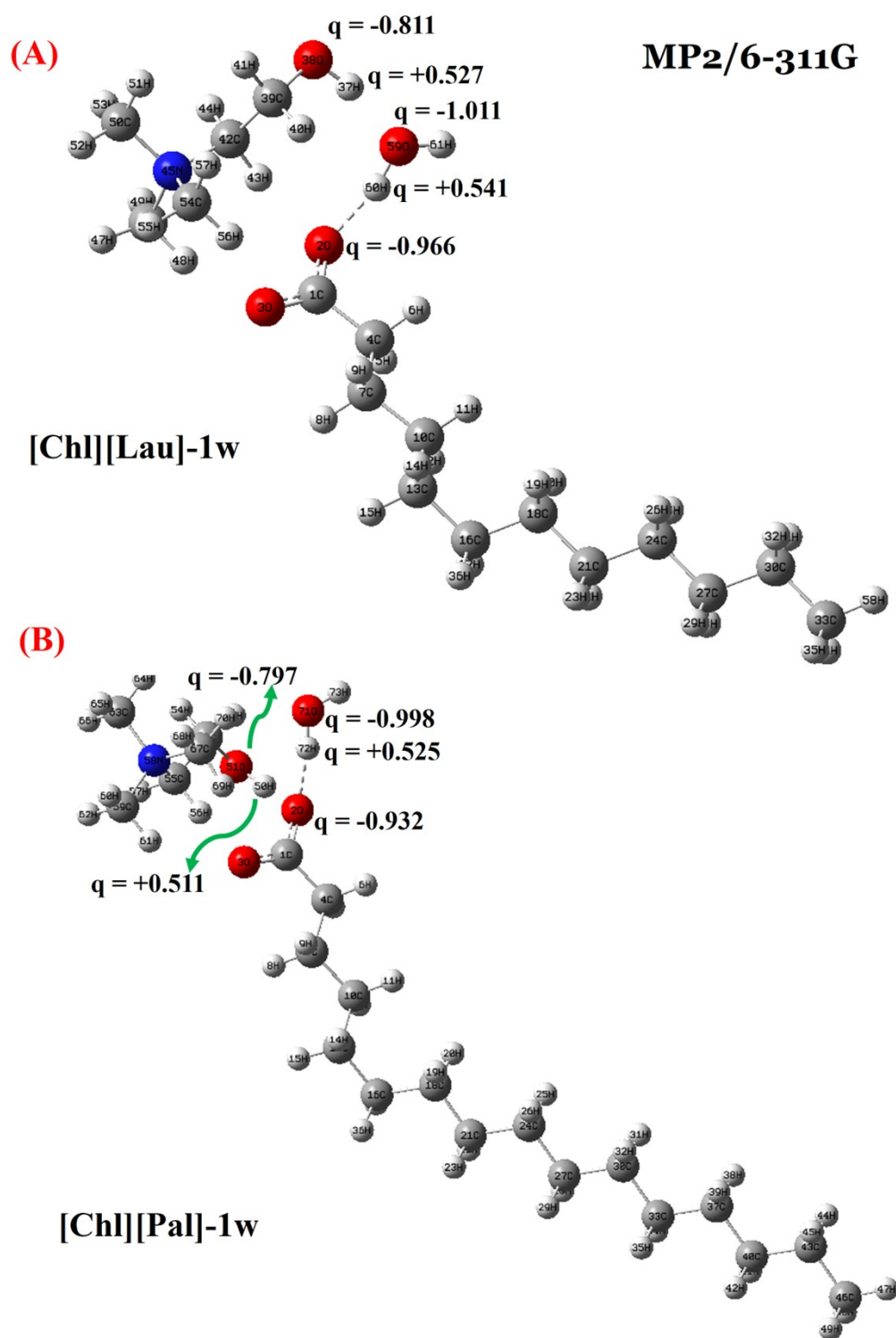
*Corresponding Authors Information:

E-mail: gardas@iitm.ac.in
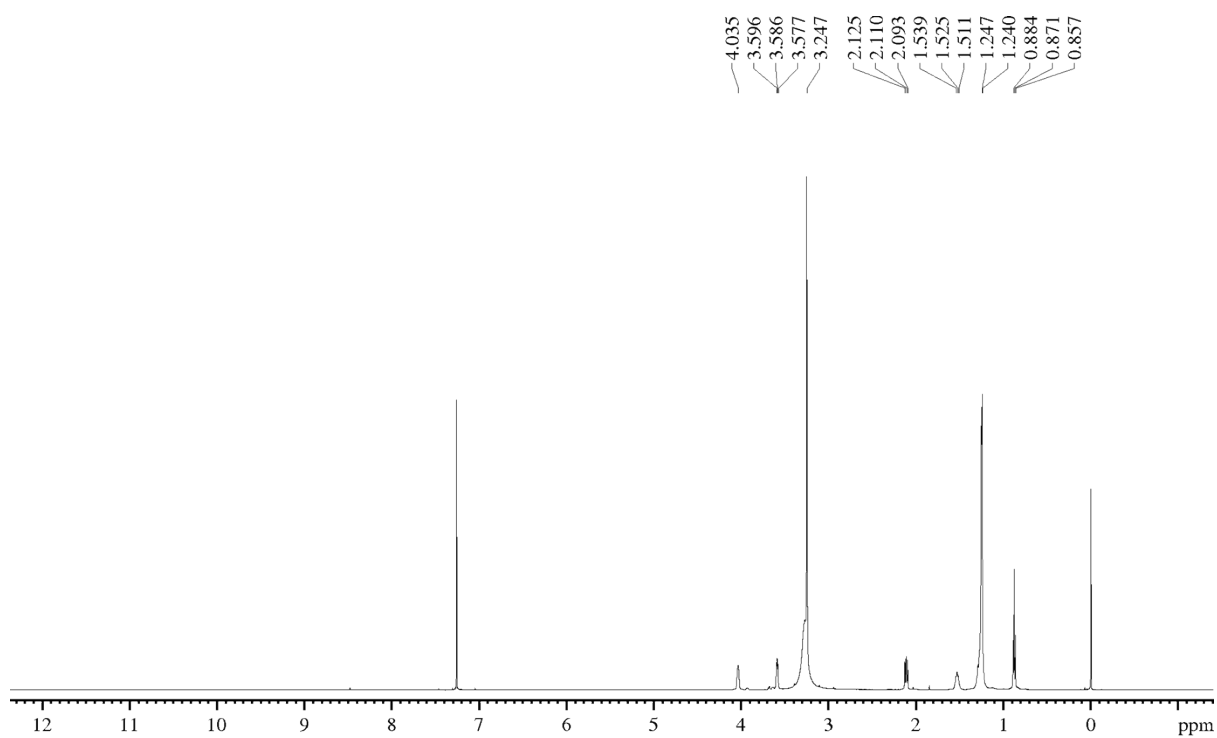
Fig. S1. ^{1}H NMR of choline laurate [Chl][Lau].

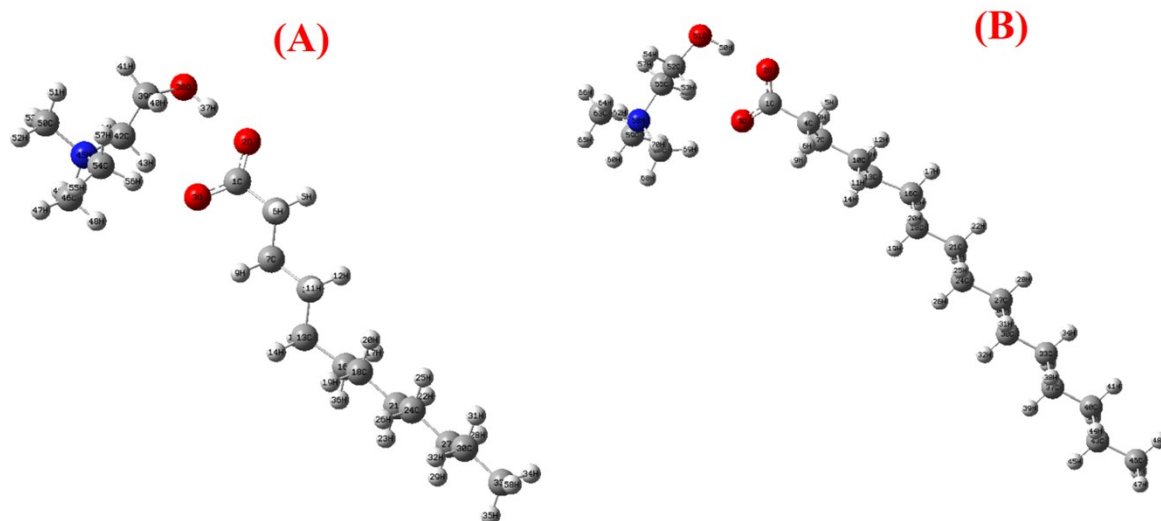**Fig. S2.** ^{1}H NMR of choline palmitate [Chl][Pal].

Fig. S3. Plot of weight per cent against temperature to illustrate the thermal decomposition of the studied SAILs.

Fig. S4. Optimized molecular structures with NBO charges for binary **(A)** [Chl][Lau]-water and **(B)** [Chl][Pal]-water systems calculated at the MP2/6-311G level of theory.
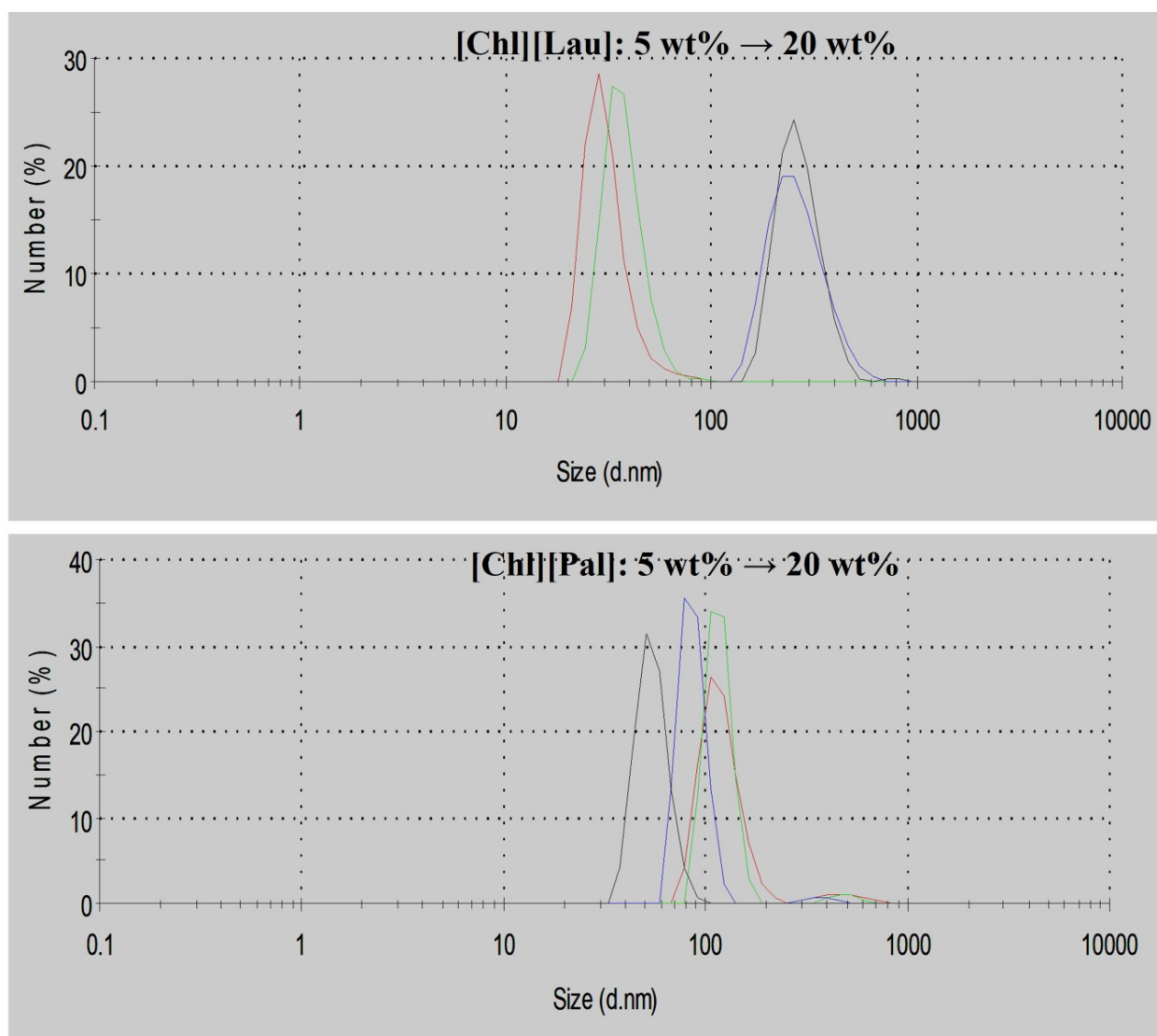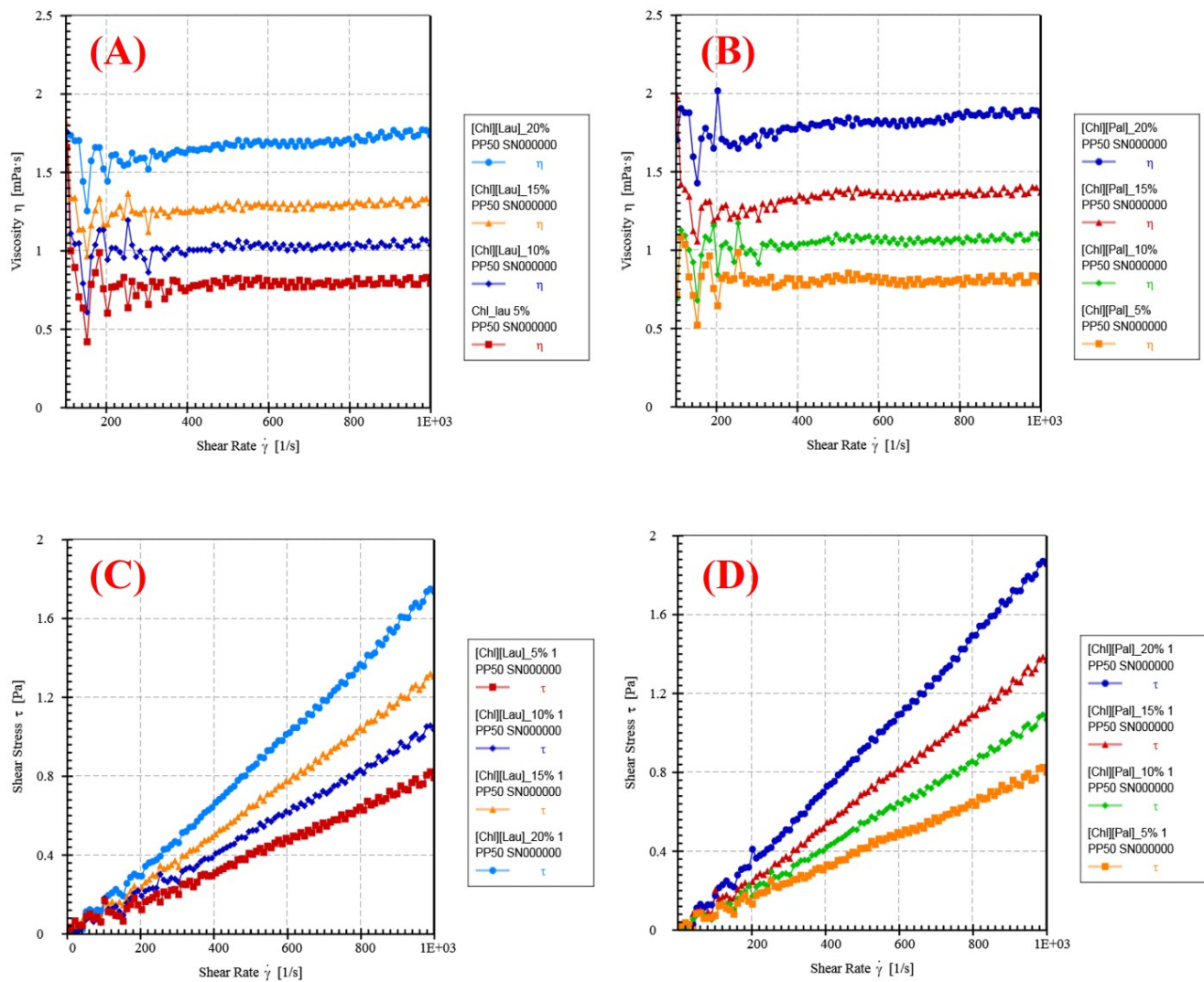
MP2/6-311G-IEFPCM with water

(A)

(B)

[Chl][Lau]: -88.083 kJ/mol   [Chl][Pal]: -87.871 kJ/mol

Fig. S5. Optimized molecular structures for **(A)** [Chl][Lau] and **(B)** [Chl][Pal] calculated using the polarizable continuum model at the MP2/6-311G level of theory.

Fig. S6. Size distribution profiles as a function of concentration of [Chl][Lau] and [Chl][Pal] in water at 303 K.

Fig. S7. Plots for the variation of viscosity (η) versus steady shear rate (γ) as a function of concentration of **(A)** [Chl][Lau] and **(B)** [Chl][Pal] in water at 303 K. Plots for the variation of shear stress (τ) versus steady shear rate (γ) at different concentration of **(C)** [Chl][Lau] and **(D)** [Chl][Pal] in water.
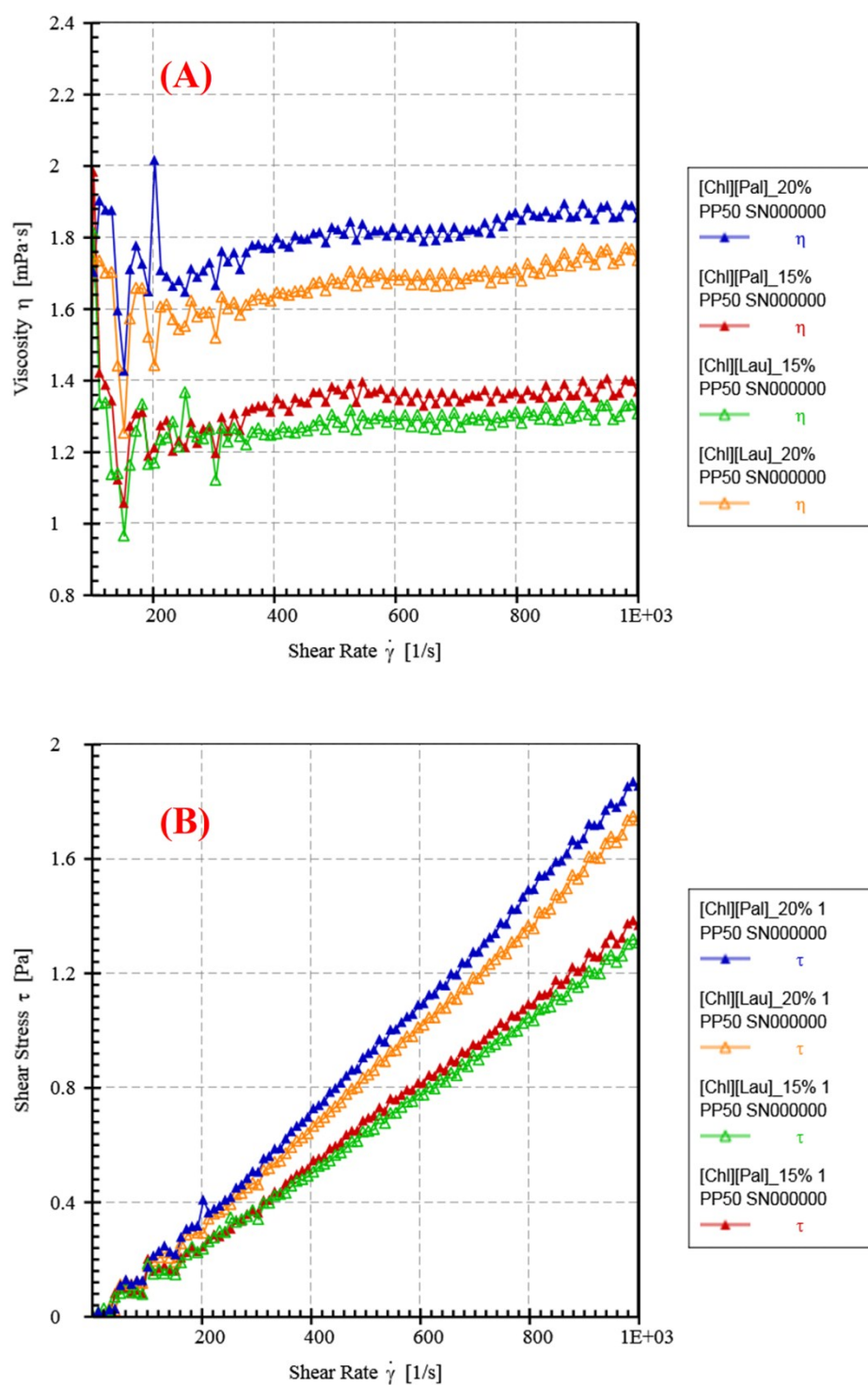
Fig. S8. Comparative plots **(A)** viscosity (η) versus steady shear rate (γ) at 15 wt% and 20 wt% concentration of [Chl][Lau] and [Chl][Pal] in water at 303 K. Comparative plots **(B)** shear stress (τ) versus steady shear rate (γ) at 15 wt% and 20 wt% concentration of [Chl][Lau] and [Chl][Pal] in water at 303 K.
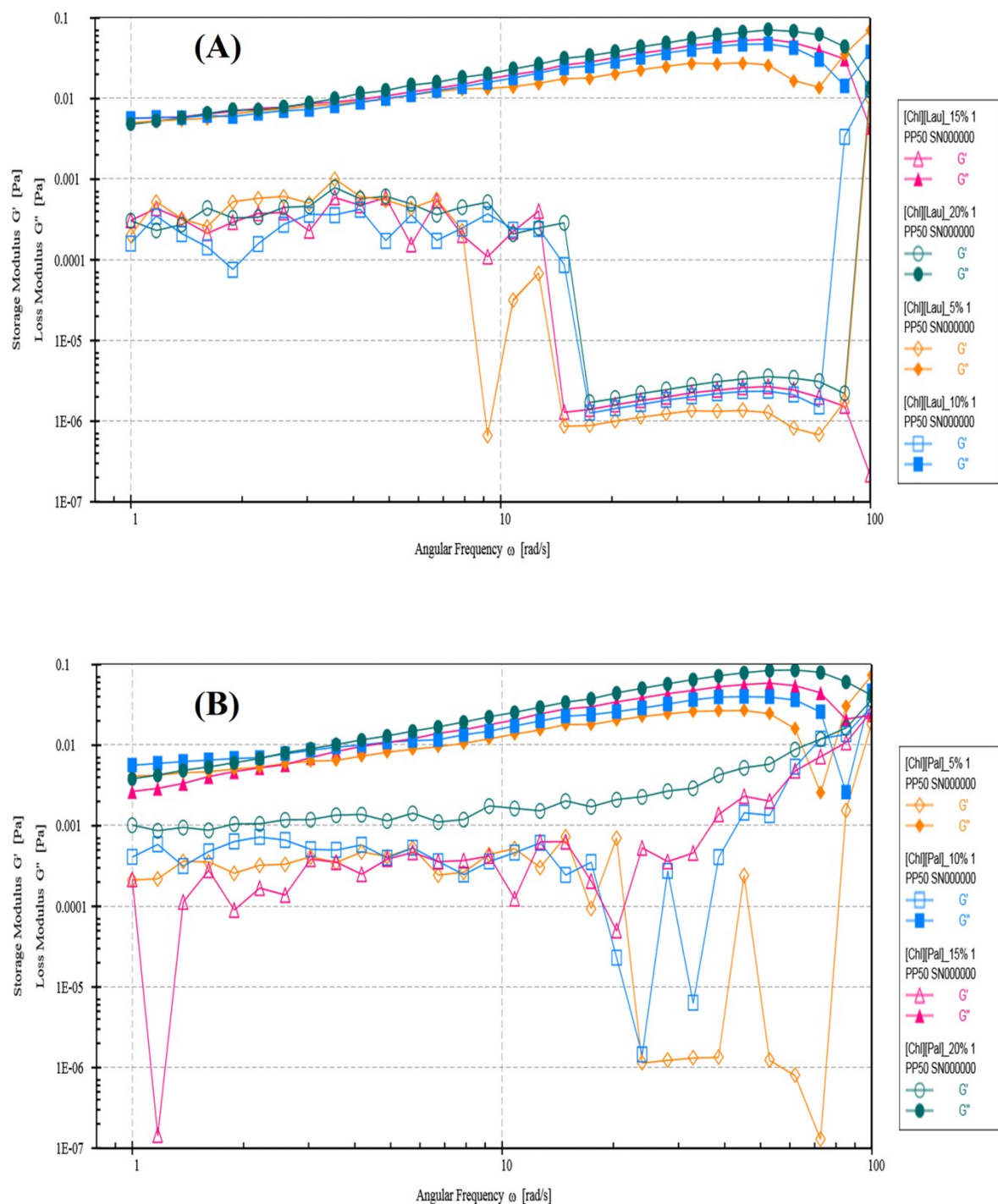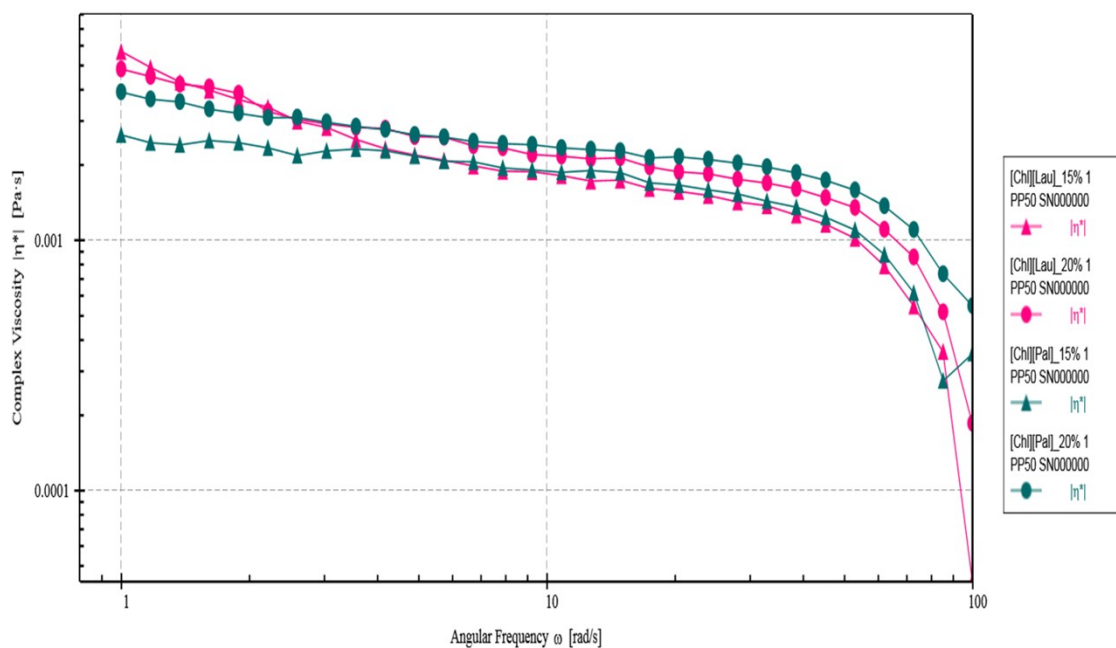
Fig. S9. Variation of the storage modulus (G′), and loss modulus (G″) relative to the angular frequency (ω) of micellar systems at 5 wt% to 20 wt% concentration of **(A)** [Chl][Lau] and **(B)** [Chl][Pal] and temperature of 303 K, where open and filled symbols correspond to G´ and G″, respectively.
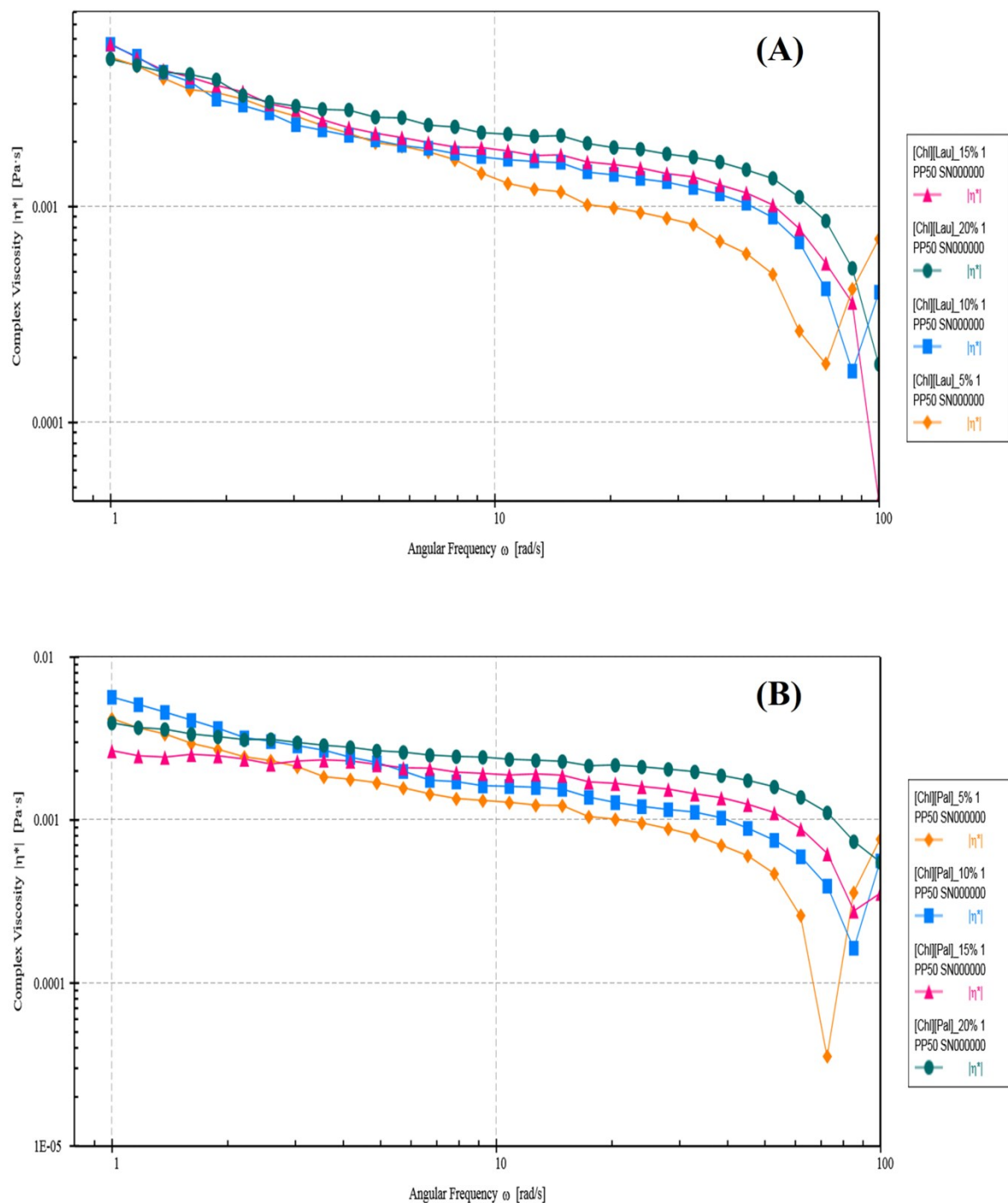
Fig. S10. Variation of the complex viscosity (|η*|) relative to the angular frequency (ω) of micellar systems at 5 wt% to 20 wt% concentration of **(A)** [Chl][Lau] and **(B)** [Chl][Pal] and temperature of 303 K.

Fig. S11. Comparative variation of the complex viscosity (|η*|) aganist angular frequency (ω) of micellar systems at 5 wt% to 20 wt% concentration of **(A)** [Chl][Lau] and **(B)** [Chl][Pal] and temperature of 303 K.
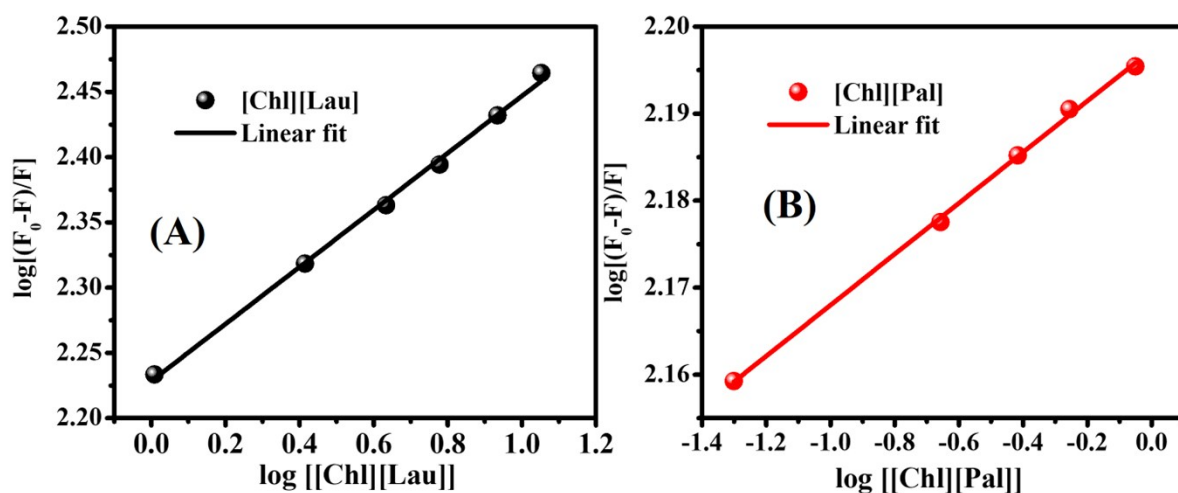
Fig. S12. Double-log plots of the **(A)** [Chl][Lau] and **(B)** [Chl][Pal] quenching effect on BSA fluorescence at 303 K.